AIAA JOURNAL
Vol. 35, No. 4, April 1997

Geometric Approach to Nondestructive Identification of Faults in Stochastic Structural Systems

M. H. Sadeghi*
University of Tabriz, Tabriz 516 66, Iran
and
S. D. Fassois†
University of Patras, Patras GR-265 00, Greece

A novel geometric approach to the nondestructive identification of faults in stochastic structural systems, based on vibration test data, is introduced. The approach uses a partial and reduced-order dynamic system model, a properly selected stochastic feature space, the notion of fault mode as the union of all faults of one particular cause, and its approximate geometric representation as a subspace of the feature space. Fault identification is accomplished by determining the fault mode subspace within which the current fault lies. The geometric approach offers important advantages over alternative structural fault identification schemes, including its inherent accommodation of stochastic effects, the use of a minimal number of measurement locations, and its ability to operate on any type of vibration data and use only partial and reduced-order models, while relaxing the need for stiffness matrix or modal parameter estimates. Its effectiveness is demonstrated via fault identification in a laboratory-scale beam and a finite element model of a planar truss structure, where the importance of stochastic effect accommodation is addressed.

I. Introduction

STRUCTURAL systems, such as buildings, bridges, offshore platforms, and aerospace structures, are amenable to structural fault and damage. If not promptly detected and identified (localized), such faults may evolve and lead to eventual catastrophic failure. Techniques for the nondestructive detection and identification of structural faults therefore are of paramount importance for reasons associated with safety and proper maintenance.[1]

In a typical structural system, degradation due to a developing fault manifests itself as a change in the system's static and dynamic properties, especially stiffness.[2] Such a change induces a corresponding change in the system's modal parameters and response characteristics. Nondestructive structural fault detection and identification thus often is based upon the study of behavioral discrepancies between the nominal (unfailed) and failed systems. As a binary decision-making problem, fault detection is typically easier to accomplish than fault identification, which is a multiple decision-making problem and the primary focus of this work.

A large category of structural fault identification methods is based upon the evaluation of changes incurred in the system's stiffness matrix, usually under the constant mass matrix assumption. These methods may use static test data,[3] dynamic test data,[4–6] or combinations of the two.[7] The main idea is in the use of the test data to formulate an optimization problem through which the changes of the structural stiffness matrix from its nominal (unfailed) value (often determined from a finite element model of the structure) are evaluated. The methods achieve simultaneous fault detection and identification based upon the determination of the changed stiffness matrix elements.

These methods are, nevertheless, characterized by a number of drawbacks and limitations: Static testing may be a problem with many (especially large) structures, whereas complete eigenmode information (required in the dynamic test case) is difficult to obtain and requires a large number of sensors and elaborate testing procedures. The determination of eigenmode information additionally requires the numerical solution of nonlinear equations. A complete structural model, though of a possibly large dimension, is necessary to estimate, and this leads to a large nonlinear optimization problem. A stiffness matrix element may have contributions from several structural elements sharing the same joint, thus rendering the precise location of the fault problematic. Stochastic effects usually are not accounted for, and may lead to additional difficulties in fault detection and identification.[6] The fact that eigenmode estimates are themselves stochastic quantities with inherent variability is not taken into account, with the result being that, oftentimes, there can be no sufficient certainty that an observed change in a stiffness parameter is due to a fault and not to the inherent variability of the data.[8]

An alternative category of methods is based upon the evaluation of changes incurred in the structural system's modal parameters.[8–10] The basic idea is the comparison of the modal parameters of the nominal system to those of the failed, and the (potential) detection and identification of faults through observation of the incurred change patterns. These methods are, nevertheless, still constrained to the deterministic domain and require modal parameter estimation, with most of them specifically requiring complete mode shape information and thus a large number of sensors and elaborate testing procedures. Even then, faults may not always be possible to properly identify from mode shape pattern changes. The method of Lew[11] relaxes the need for complete mode shape information, but remains essentially deterministic and limited to fixed-magnitude (degree of severity) faults.

In this work, a novel geometric approach to the nondestructive identification of faults in stochastic structural systems, based upon vibration test data, is introduced. This approach makes use of a partial and reduced-order stochastic structural system model; a proper feature vector; a corresponding stochastic feature space equipped with a proper metric; and the notion of fault mode as the union of faults of all possible magnitudes but of common cause, along with its approximate geometric representation as a subspace of the feature space.

The approach is based on the fact that fault-induced changes in the structural system's properties affect the model parameters, and through them, the feature vector statistical characteristics.

Within the selected feature space all individual (fixed-magnitude) faults assume a pointwise representation, whereas each fault mode is represented as a proper subspace. Approximate representations of these subspaces are preconstructed in a training stage. Once a system fault is detected through the use of statistical detection techniques, an

Received Feb. 1, 1996; revision received Oct. 26, 1996; accepted for publication Jan. 7, 1997.

*Faculty of Mechanical Engineering.
†Associate Professor, Faculty of Mechanical and Aeronautics Engineering.

interval (mean and covariance) estimate of the current feature vector, defining its point representation in the feature space, is obtained. Fault identification then is accomplished by determining the specific fault mode subspace within which the current fault point lies.

The proposed approach is distinctly different from previous schemes for the following reasons.

1) It is inherently stochastic and thus effective in separating fault-induced effects from those due to environmental factors and the variability of the test data.

2) It requires a minimal number of measurement locations.

3) It is capable of operating on any type (acceleration, velocity, or displacement) of vibration test data.

4) It requires the estimation of a very simple partial and reduced-order structural model and no modal parameter information.

In addition, it avoids the solution of a large nonlinear optimization problem, it is capable of identifying faults other than those related to stiffness changes, and it is not necessarily restricted to linear viscously damped structures but may be actually used with any linear or nonlinear type of structure.

The rest of this paper is organized as follows. The main ideas and procedures of the geometric fault identification approach are presented in Sec. II. Its use for the identification of faults in a laboratory-scale simply supported beam and a finite element model of a planar truss structure is discussed in Secs. III and IV, respectively, and the conclusions of this study are summarized in Sec. V.

II. Geometric Fault Identification Approach

A. Basic Ideas

The elements composing the geometric fault identification approach are 1) a partial and reduced-order mathematical system model, 2) a properly selected feature vector, 3) a feature space equipped with a proper metric, and 4) the notion of fault mode and its geometric representation.

The mathematical system model is of the discrete-time stochastic dynamic type, providing a partial and reduced-order representation of the actual structure. These representation characteristics are very important not only because a complete system model may be difficult to construct but also because it may be difficult, or impractical, to use. The model typically is obtained through identification techniques using vibration test data.[12–14]

The feature vector, consisting of selected model parameters, is a vector "rich" in system information.

The feature space is a ρ-dimensional space spanned by the first- and, perhaps, second-order statistical characteristics of the feature vector and equipped with a proper metric.

The notion of fault mode refers to the union of faults of all possible magnitudes (degrees of severity) but common cause, for instance, those due to degradation of stiffness in a particular structural element. Within this context, a particular fault from fault mode i and of magnitude a is represented as F_a^i, with the ith fault mode thus formally defined as $F^i = \{F_a^i \mid a \in A \subseteq \Re\}$ in the one-dimensional fault magnitude case.

Within the selected feature space, all individual (fixed-magnitude) faults assume a pointwise representation. A fault mode, being a continuum of variable-magnitude faults, assumes, on the other hand, a subspace representation. The dimensionality of this subspace depends on the dimensionality of the fault magnitude, which may not be possible to always define accurately.

B. Main Operational Stages

The geometric fault identification approach is based on vibration test data, typically force excitation along with the resulting vibration displacement, velocity, or acceleration, measured at selected locations. Its main operational stages can be outlined as follows.

In an initial training stage, and with the aid of measurements obtained from a detailed simulation (typically finite element) model of the structure, a partial and reduced-order nominal system model is obtained, and a proper feature vector and corresponding feature space are selected. In addition, approximate geometric representations of the various fault mode subspaces are constructed based upon training data (obtained by injecting faults of various magnitudes into the simulation model) and appropriate regression techniques.[15]

Once the presence of a system fault is detected based on periodically obtained actual vibration system data and statistical fault detection schemes, an interval (mean and covariance) estimate of the current feature vector, defining a point that represents the current (unknown) fault in the feature space, is obtained. The fault identification problem then is viewed as the problem of determining the specific fault mode subspace within which the occurred fault lies.

A technical difficulty encountered in this context is that, because of estimation and modeling inaccuracies, the point representing the current fault may not strictly belong to its proper subspace but to its immediate vicinity. To account for this, the fault identification problem is formulated as a geometric minimal distance one, according to which the current fault is associated with the fault mode with the subspace of which its distance (computed via a constrained optimization scheme) is minimal.

For purposes relating to practical use and computational simplicity, the fault mode subspace representations are approximated as linear $(\rho - 1)$-dimensional (overspecified) subspaces that include the actual fault modes. The implications of these approximations may need to be assessed in practice; yet, justification of the linearity approximation may be offered for limited ranges of fault magnitudes, and subspace overspecification is not expected to appreciably affect the decision-making process because the estimated fault points should always lie in the vicinity of their corresponding modes.

The stages of the geometric approach thus may be formally presented as follows.

1. *Feature Space Selection and Fault Mode Subspace Construction (Training Stage)*

Based on data obtained from a detailed simulation model, the structure and interval parameter estimates of a partial and reduced-order system model are obtained through suitable identification techniques.[12–14] Let θ denote the selected feature vector, viewed as a stochastic quantity with mean μ_θ and covariance P_θ.

A ρ-dimensional (stochastic) feature space is selected as the space spanned by the first-order and, perhaps, certain or all of the second-order moments of the feature vector. Let these selected elements compose the ρ-dimensional vector θ_K.

Additional experiments, in which p faults of various magnitudes are, for each one of the, say, N_F fault modes injected into the detailed simulation model, are performed, and the corresponding estimates θ_K^{ij} obtained. In this notation, i_j refers to the jth fault ($j = 1, \ldots, p$) within the ith fault mode ($i = 1, \ldots, N_F$).

For purposes of computational simplicity, the fault mode representations are approximated as linear $(\rho - 1)$-dimensional subspaces (hyperplanes). The mathematical form of the ith fault mode hyperplane is

$$g^i(\theta_K) = \theta_{K_1} + \omega_1^i \theta_{K_2} + \ldots + \omega_{\rho-1}^i \theta_{K_\rho} - \omega_\rho^i = 0$$

$$\Rightarrow (\bar{\omega}^i)^T \theta_K - \omega_\rho^i = \theta_{K_1} + \bar{\theta}_K^T \cdot \omega^i = 0 \tag{1}$$

with ω_l^i denoting the hyperplane's lth coefficient and

$$\omega^i = [\omega_1^i \;\; \omega_2^i \;\; \ldots \;\; \omega_\rho^i]^T \qquad \bar{\omega}^i = [1 \;\; \omega_1^i \;\; \ldots \;\; \omega_{\rho-1}^i]^T \tag{2}$$

$$\theta_K = [\theta_{K_1} \;\; \theta_{K_2} \;\; \ldots \;\; \theta_{K_\rho}]^T \qquad \bar{\theta}_K = [\theta_{K_2} \;\; \ldots \;\; \theta_{K_\rho} \;\; -1]^T \tag{3}$$

Given the ith ($i = 1, \ldots, N_F$) fault mode estimates θ_K^{ij} ($j = 1, \ldots, p$) with $p > \rho$, the corresponding hyperplane representation is estimated through linear regression using expressions of the form

$$\theta_{K_1}^{ij} + (\bar{\theta}_K^{ij})^T \cdot \omega^i = \epsilon^{ij} \qquad (1 \le j \le p) \tag{4}$$

in which ϵ^{ij} denotes the jth regression error. These lead to the estimator

$$\hat{\omega}^i = -[(\bar{\theta}_K^i)^T \bar{\theta}_K^i]^{-1} \cdot (\bar{\theta}_K^i)^T \theta_{K_1}^i \tag{5}$$

where

$$\bar{\theta}_K^{i} \triangleq \begin{bmatrix} (\bar{\theta}_K^{i_1})^T \\ (\bar{\theta}_K^{i_2})^T \\ \vdots \\ (\bar{\theta}_K^{i_p})^T \end{bmatrix} \tag{6}$$

and

$$\theta_{K_1}^{i} = \left[\theta_{K_1}^{i_1} \quad \theta_{K_1}^{i_2} \quad \ldots \quad \theta_{K_1}^{i_p}\right]^T \tag{7}$$

□

2. Current Feature Vector Estimation

Once a fault is detected, based on periodically obtained structural system vibration data, an interval estimate of the current (unknown fault) feature vector θ^{μ} is obtained. □

3. Distance Computations

Appropriate distances between the current (unknown fault) point θ_K^{μ} and each fault mode hyperplane are subsequently computed. The distance between θ_K^{μ} and the ith mode hyperplane is obtained by optimizing the Lagrangian

$$L(\theta_K, \gamma) = D(\theta_K, \theta_K^{\mu}) + 2\gamma \cdot g^i(\theta_K) \tag{8}$$

with respect to θ_K and γ. In the preceding, $D(\cdot, \cdot)$ represents an appropriate distance function (metric), 2γ the Lagrange multiplier, and $g^i(\theta_K)$ the ith mode hyperplane defined by Eq. (1). □

C. Feature Space and Distance Function Selection

The metrics used determine the nature of the feature space and the composition of the vector θ_K. Three possibilities are considered.

1. Deterministic Metric Space

In this case, $\theta_K = \mu_\theta$, that is, only the mean of the feature vector is used, and

$$D(\theta_K, \theta_K^{\mu}) = \mathrm{tr}\left\{(\mu_\theta - \mu_{\theta^{\mu}})(\mu_\theta - \mu_{\theta^{\mu}})^T\right\} \tag{9}$$

with $\mathrm{tr}\{\}$ denoting trace of the indicated matrix quantity. □

2. Stochastic Metric Space

In this case, $\theta_K = [\mu_\theta^T, (\mathrm{col\,diag}\, P_\theta)^T]^T$, that is, the mean and the diagonal of the feature vector covariance are used, and

$$D(\theta_K, \theta_K^{\mu}) = \mathrm{tr}\left\{(\mu_\theta - \mu_{\theta^{\mu}})(\mu_\theta - \mu_{\theta^{\mu}})^T + (\boldsymbol{s}_\theta - \boldsymbol{s}_{\theta^{\mu}})(\boldsymbol{s}_\theta - \boldsymbol{s}_{\theta^{\mu}})^T\right\} \tag{10}$$

with $\mathrm{col\,diag}(\,)$ denoting the column vector consisting of the diagonal elements of the indicated matrix and $\boldsymbol{s}_\theta$ the vector of the standard deviations of the elements of θ. □

3. Kullback Pseudometric Space

In this case $\theta_K = [\mu_\theta^T, (\mathrm{col}\, P_\theta)^T]^T$, that is, the whole feature vector covariance matrix is used in connection with the Kullback pseudodistance function (J-divergence distance) defined as[16]

$$D(\theta_K, \theta_K^{\mu}) = \int \left[f_{\theta_K}(\lambda) - f_{\theta_K^{\mu}}(\lambda)\right] \cdot \ln \frac{f_{\theta_K}(\lambda)}{f_{\theta_K^{\mu}}(\lambda)} \cdot d\lambda \tag{11}$$

where $f_{\theta_K}(\lambda)$, $f_{\theta_K^{\mu}}(\lambda)$ denote the probability density functions of the random vectors θ_K and θ_K^{μ}, respectively. In the Gaussian case, this expression results in

$$D(\theta_K, \theta_K^{\mu}) = \frac{1}{2}\left\{\mathrm{tr}\left[(P_{\theta^{\mu}} - P_\theta)(P_\theta^{-1} - P_{\theta^{\mu}}^{-1})\right] + \mathrm{tr}\left[(\mu_{\theta^{\mu}} - \mu_\theta)(P_{\theta^{\mu}}^{-1} + P_\theta^{-1})(\mu_{\theta^{\mu}} - \mu_\theta)^T\right]\right\} \tag{12}$$

□

In comparing these spaces, it is remarked that the first one is best suited for the special case of purely deterministic systems, or systems operating in very-low-noise environments, and leads to a quadratic optimization problem admitting a closed-form solution. The other two are appropriate for the broader class of stochastic structural systems. The stochastic metric space makes use of partial covariance information (variances of the feature vector elements), whereas the Kullback pseudometric space uses the full covariance matrix. From a computational standpoint the former leads to a quadratic optimization problem as well, whereas the latter requires the use of nonlinear optimization techniques, such as the iterative gradient algorithm.[17]

III. Fault Identification in a Simply Supported Beam

A. Objectives and Description of Experimental Setup

The geometric approach is used for the identification of faults in a laboratory-scale beam. The beam is based on four rigid supports, dividing it into three spans, and two additional flexible supports—one stationary, referred to as auxiliary spring, and one movable that is at the midpoint of the central span in the nominal (unfailed) system case and is referred to simply as spring (Fig. 1).

The faults considered are deviations of the local stiffness characteristics (local changes in the modulus of elasticity) realized by transporting the movable support (spring) to any desired point in any span.

The objective of the experiments is fault detection and identification, with the latter term implying the determination of the span in which a particular fault occurs, based upon vibration test data. To minimize the necessary equipment and signal-processing requirements, fault detection and identification are based on a single pair of measurements.

The experimental setup thus consists of a shaker applying a vertical force (a realization of a zero-mean and uncorrelated stochastic process) at a point close to the left end of the beam, a load cell measuring the exerted force, and a proximity probe measuring the resulting vertical vibration displacement at the midpoint of the central span (Fig. 1). The measured force and vibration displacement signals are driven through analog antialias filters, digitized at a sampling frequency of 1 kHz, and stored in a personal computer for further processing. Sample normalized versions of both are, for the nominal (unfailed) system case, shown in Fig. 2.

Fault identification thus is based upon a partial (single transfer function) system model, with no regard to mode shape information. Note that this particular experimental setup, in which fault magnitude is simulated by changing the fault specific position within a considered span, makes fault identification difficult because faults realized at a continuum of positions across spans (and thus belonging to different fault modes) correspond to a continuum of changes in the elasticity characteristics of the considered transfer function.

B. Preliminary Procedures

For the stochastic mathematical description of the transfer function characteristics, a parametric autoregressive moving average with exogenous excitation (ARMAX) representation[13] is used. Preliminary analysis of nominal system data via both nonparametric

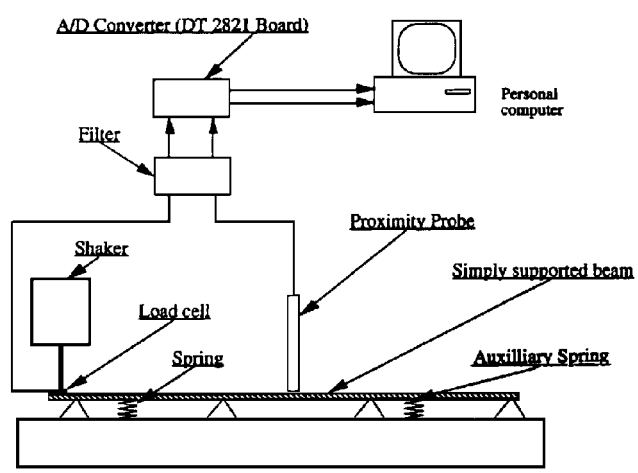

Fig. 1 Schematic diagram of simply supported beam experimental setup.

Table 1 Fault detection [$Q(K)$] and identification (stochastic distance) results[a]

Faults	Test case	$Q(K)$	Stochastic distance from hyperplane F^1	F^2	F^3
No fault	0	28.74	—	—	—
F^1 (span 1)	1	940.96	**2.0647e_05**	4.5498e_03	5.0656e_03
	2	776.18	2.2660e_03	**1.3047e_03**	8.5332e_03
	3	696.42	**8.3229e_05**	1.1996e_02	1.7795e_02
	4	549.26	**2.2866e_03**	1.1940e_02	5.4363e_03
	5	740.11	**4.4298e_03**	1.7443e_02	1.3721e_02
	6	883.60	**1.5372e_03**	4.0091e_03	1.1468e_02
F^2 (span 2)	7	253.03	9.0472e_03	**7.6697e_03**	2.1568e_02
	8	293.17	8.6767e_03	**8.8407e_04**	1.3893e_02
	9	290.15	1.4295e_02	**1.2209e_03**	1.6875e_02
	10	404.02	8.9338e_03	**1.9721e_03**	1.5435e_02
	11	497.78	1.6199e_02	**1.0132e_03**	1.8786e_02
	12	446.56	1.0375e_02	**1.7487e_03**	1.3981e_02
F^3 (span 3)	13	922.73	5.9409e_03	3.1545e_03	**8.3204e_04**
	14	906.81	3.5360e_03	1.5654e_03	**8.9274e_04**
	15	584.43	3.9264e_03	3.6697e_03	**3.1019e_04**
	16	642.12	4.1098e_03	1.0040e_03	**6.1854e_04**
	17	606.36	2.9405e_03	5.6205e_03	**1.4935e_03**
	18	490.66	3.4288e_03	8.9146e_03	**9.5780e_04**

[a]Geometric approach using the stochastic metric space; minimal distance in each test case is indicated by boldface (beam).

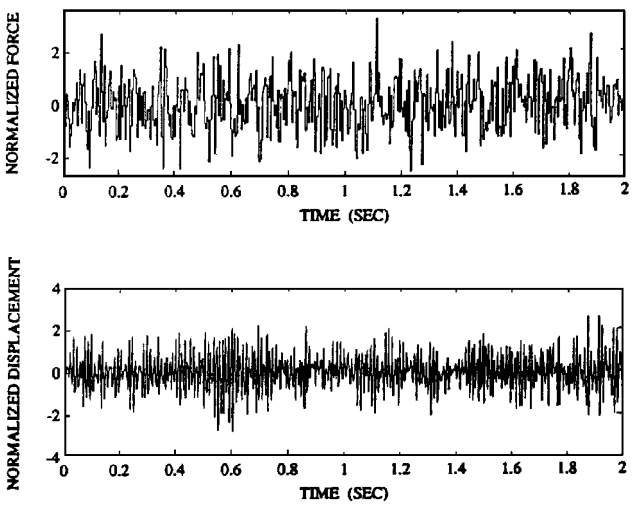

Fig. 2 Sample normalized force excitation and vibration displacement signals (simply supported beam).

and parametric identification techniques indicates that the beam is characterized by four vibrational modes in the 0–400-Hz frequency range; yet, for purposes of computational simplicity, a reduced-order ARMAX (6, 5, 3) model accounting for only three of the modes is estimated on the basis of 1500-sample-long data records. This model is of the form

$$\sum_{i=0}^{6} a_i \cdot y[t-i] = \sum_{i=0}^{5} b_i \cdot F[t-i] + \sum_{i=0}^{3} c_i \cdot w[t-i]$$

with $a_0 \triangleq c_0 \triangleq 1$, $y[t]$ representing the measured vibration displacement, $F[t]$ the exerted force signal, $w[t]$ a zero-mean and uncorrelated noise-generating stochastic sequence, and a_i, b_i, c_i the ith autoregressive (AR), exogenous (X), and moving average (MA) parameter, respectively.

The feature vector is selected to consist of the model's AR and X parameters, that is,

$$\theta = [a_1 \quad \dots \quad a_6 \mid b_1 \quad \dots \quad b_5]^T$$

while all three feature spaces of Sec. II.C are considered. The deterministic feature space is spanned by the elements of the feature vector mean, the stochastic feature space is additionally spanned by their variances, and the Kullback pseudometric space further adds off-diagonal covariance information.

Three fault modes, denoted as F^1, F^2, and F^3 and corresponding to changes in the local stiffness characteristics at a point lying respectively, anywhere in the first, second, and third span of the beam, are considered. The fault mode hyperplanes are constructed according to the procedure of Sec. II.B, by realizing faults at various points of each span.

C. Results and Discussion

Nineteen test cases, the first one (zeroth) corresponding to the unfailed state of the system, and each one of the subsequent 18 (1st–18th) corresponding to a particular fault (fault location) from one of the three fault modes, are considered. Test cases 1–6 correspond to faults belonging to fault mode F^1 (realized by inserting the spring at the positions $L/24$, $2L/24$, $3L/24$, $5L/24$, $6L/24$, $7L/24$, with L denoting the length of the beam between the left and right rigid supports); the next six (7–12) to faults belonging to fault mode F^2 (spring at $9L/24$, $10L/24$, $11L/24$, $13L/24$, $14L/24$, $15L/24$); and the last six (13–18) to faults belonging to fault mode F^3 (spring at $17L/24$, $18L/24$, $19L/24$, $21L/24$, $22L/24$, $23L/24$). Note that, to test the robustness of the approach with respect to specific fault location within a span, none of these fault locations were used in the hyperplane construction (training) stage.

The fault detection and identification results are presented in Table 1, with each row representing each one of the 19 test cases.

Fault detection is based upon a portmanteau lack-of-fit test[12] on the residuals (one-step-ahead prediction errors) generated by the nominal (unfailed) ARMAX model driven by the measured, in each case, force excitation and vibration displacement signals. The test uses the statistic

$$Q(K) = N \cdot \hat{r}_{ee}^{-2}[0] \cdot \sum_{i=1}^{K} \hat{r}_{ee}^{2}[i] \tag{13}$$

in which N represents the number of data samples used in evaluating the residuals, K the number of autocorrelation terms used, and $\hat{r}_{ee}[i]$ the estimate of the residual normalized autocorrelation function at lag i. Asymptotically (as $N \to \infty$) $Q(K)$ follows a chi-squared distribution with K degrees of freedom. Hence, the null hypothesis (H_0) that the residual sequence is uncorrelated, and thus the nominal model is still valid, is accepted at the α significance level (that is, the probability of rejecting H_0 when H_0 actually holds is equal to α) if $Q(K) < \chi^2_{1-\alpha}(K)$, whereas it is rejected if $Q(K) > \chi^2_{1-\alpha}(K)$. In these expressions $\chi^2_{1-\alpha}(K)$ represents the $1-\alpha$ percentile of the chi-squared distribution with K degrees of freedom, defined such that $\text{Prob}[X < \chi^2_{1-\alpha}(K)] = 1-\alpha$.

The statistic $Q(K)$ (Table 1, column 3) is in the zeroth test case smaller than its threshold value of 31.3 ($\alpha = 0.005$, $K = 14$) and thus correctly indicating no fault occurrence. In all subsequent

(1st–18th) cases, $Q(K)$ is greater than its threshold value, thus correctly detecting fault occurrence.

The fault identification results (Table 1, columns 4–6) are obtained with the geometric approach using the stochastic metric space. The computed distances of the current (unknown fault) point from each fault mode hyperplane are presented, with the minimal one in each test case indicated in boldface. Despite the difficulties of this particular setup and the use of a single transfer function model, the identification results are very satisfactory, with only one misclassification error encountered (test case 2).

The behavior of the geometric approach in conjunction with the Kullback pseudometric space is quite similar (two misclassification errors), but a deterioration is observed when the deterministic metric space is used (five misclassification errors). This is due to the inadequacy of the deterministic metric space in this context, and underscores the importance of using the stochastic spaces in conjunction with systems characterized by nonnegligible (for instance, standard deviation noise-to-signal ratios of 1% or higher) random effects. Between the two stochastic spaces, the stochastic metric one is, from a computational standpoint, preferable.

IV. Fault Identification in a Truss Structure

A. Objectives and Description of Setup

In this section the geometric approach is used for the identification of faults in a finite element model of a planar truss structure consisting of 16 elements (steel bars) connected at 10 joints.

A schematic diagram of the structure, along with that of its finite element model representation is shown in Fig. 3. Although a consistent (nondiagonal) mass matrix is used in the actual finite element model, the masses are, for purposes of illustration simplicity, shown as lumped (Fig. 3b). The length of the elements 1–8, 10, 12, 14, and 16 is $L = 5 \times 10^{-1}$ m, whereas that of the elements 9, 11, 13, and 15 is $L = 5\sqrt{2} \times 10^{-1}$ m. Their cross-sectional area is $A = 4 \times 10^{-4}$ m^2, their specific mass is $\rho = 7860$ kg/m^3, and their modulus of elasticity is $E = 200$ GPa. The structural damping is of the proportional type, with the damping matrix being 2% of that of the stiffness. The vibration response is computed by integrating the equations of motion using the Newmark integration method[18] and an integration step of 0.001 s.

The faults considered are deviations of the local stiffness characteristics (modulus of elasticity) of the various structural elements (bars).

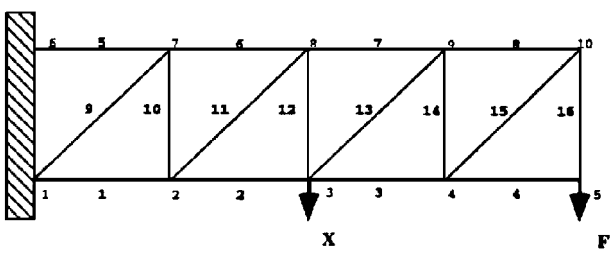

a) Schematic diagram

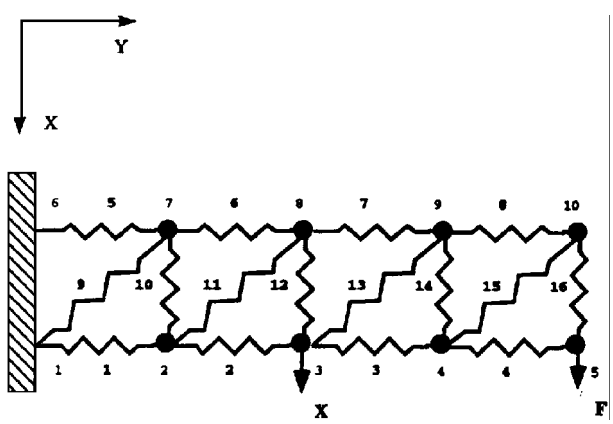

b) Finite element model

Fig. 3 Planar truss structure.

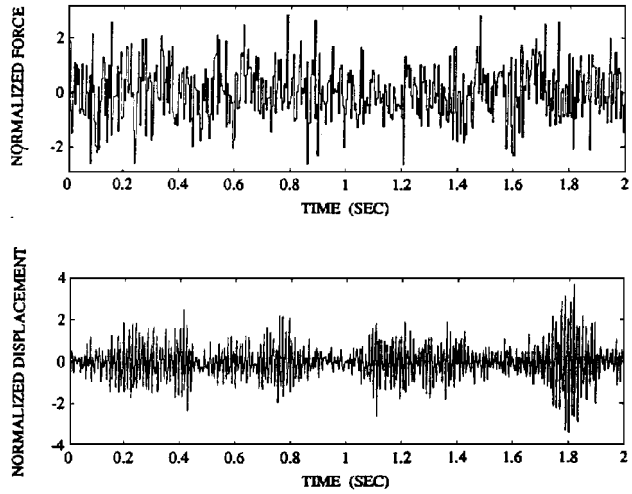

Fig. 4 Sample normalized force excitation and vibration displacement signals (planar truss structure).

The objective of the experiments is fault detection and identification, with the latter term implying the determination of the particular element (bar) in which a fault occurs, based on vibration test data.

As in the beam case, to minimize the necessary equipment and signal-processing requirements, fault identification is based on a single pair of vibration measurements: measurement of the stochastic (zero-mean and uncorrelated) force excitation applied at joint 5 along the x direction; and the resulting vibration displacement, along the same direction, at joint 3. Sample normalized versions of both measurements are, for the nominal (unfailed) system case, shown in Fig. 4.

B. Preliminary Procedures

Preliminary analysis of nominal system data, as well as the finite element model itself, indicates that the structure is characterized by three vibrational modes (at about 92.2, 337.5, and 408.9 Hz) in the 0–450-Hz range. The use of model order determination and parameter estimation techniques[13,14] in conjunction with the ARMAX model form and 1500-sample-long data records, lead to an ARMAX (6, 5, 0), that is, an ARX(6, 5) representation:

$$\sum_{i=0}^{6} a_i \cdot y[t-i] = \sum_{i=1}^{5} b_i \cdot F[t-i] + w[t]$$

with $a_0 \triangleq 1$, for the nominal (unfailed) system.

The feature vector is selected to consist of the model's AR and X parameters, that is,

$$\theta = [a_1 \quad \ldots \quad a_6 \mid b_1 \quad \ldots \quad b_5]^T$$

while all three feature spaces of Sec. II.C are considered. Four fault modes, each one corresponding to faults occurring in each one of the four elements of the upper part of the truss, are considered in the present study: Fault mode F^1 consists of the faults of all possible magnitudes occurring in element 5, F^2 of those occurring in element 6, F^3 of those occurring in element 7, and F^4 of those occurring in element 8. The corresponding fault mode hyperplanes are constructed according to the procedure of Sec. II.B.

C. Results and Discussion

Seventeen test cases, the first one (zeroth) corresponding to the unfailed state of the system and each one of the subsequent 16 (1st–16th) corresponding to a particular fault from one of the four fault modes, are considered. As in the beam experiment, none of the considered fault magnitudes was used in the hyperplane construction stage.

The fault detection and identification results are summarized in Table 2, with each row representing each one of the 17 test cases.

Fault detection is based on the portmanteau lack-of-fit test on the residuals generated by the nominal (unfailed) ARX model

Table 2 Fault detection [$Q(K)$] and identification (stochastic distance) results[a]

Faults	Test case	$Q(K)$	Stochastic distance from hyperplane F^1	F^2	F^3	F^4
No fault	0	22.71	—	—	—	—
F^1 (element 5)	1	9.9361*e*+12	**2.0559e_04**	3.6625*e*+00	1.7266*e*_01	1.8198*e*_02
	2	3.3958*e*+09	**3.2574e_04**	2.0185*e*+00	8.8179*e*_02	3.4842*e*_03
	3	3.5117*e*+07	**7.1078e_05**	9.5295*e*_01	3.9174*e*_02	8.9333*e*_04
	4	4.1011*e*+04	**1.0271e_04**	2.0369*e*_01	8.3117*e*_03	1.2304*e*_04
F^2 (element 6)	5	4.8496*e*+08	7.4069*e*_01	**6.9414e_04**	7.2368*e*_03	1.5506*e*_02
	6	6.6966*e*+05	3.8190*e*_01	1.0028*e*_02	**1.3926e_03**	8.5169*e*_02
	7	8.8924*e*+03	1.2265*e*_01	**1.3363e_04**	2.6743*e*_04	2.2007*e*_02
	8	9.8464*e*+03	8.2425*e*_03	**3.9327e_05**	2.4331*e*_04	5.2994*e*_04
F^3 (element 7)	9	4.4499*e*+08	7.9524*e*_01	7.8807*e*_03	**1.6930e_05**	1.2534*e*_02
	10	5.4150*e*+05	1.0430*e*+00	5.2164*e*_02	**1.0105e_04**	1.6928*e*_02
	11	7.8218*e*+03	1.0801*e*_01	8.2431*e*_03	**1.7911e_05**	2.3729*e*_03
	12	9.1897*e*+03	1.0190*e*_02	4.2947*e*_04	**2.8426e_05**	4.4989*e*_04
F^4 (element 8)	13	4.7348*e*+09	6.1337*e*+00	9.7726*e*_01	2.7866*e*_01	**1.3070e_05**
	14	2.3306*e*+09	1.5504*e*+00	7.0137*e*_01	1.3744*e*_01	**1.4129e_04**
	15	1.6676*e*+07	8.6585*e*_02	4.2756*e*_01	6.4683*e*_02	**4.1002e_04**
	16	1.4075*e*+04	1.1988*e*_01	1.2147*e*_01	1.2781*e*_02	**3.0925e_05**

[a]Geometric approach using the stochastic metric space; the minimal distance is, in each test case, indicated in boldface (truss).

driven by the measured, in each case, force excitation and vibration displacement signals. The statistic $Q(K)$ (Table 2, column 3) is in the zeroth test case smaller than its threshold value of 26.8 ($\alpha = 0.005$, $K = 11$), thus correctly indicating no fault occurrence. In all subsequent (1st to 16th) cases, $Q(K)$ takes values that are drastically greater than the threshold, thus again correctly detecting fault occurrence.

The fault identification results are obtained by the geometric approach, using the stochastic metric space. The computed distances of the current (unknown fault) point from each fault mode hyperplane are presented in columns 4–7 of Table 2, with the minimal one in each test case indicated in boldface. Despite the use of a single transfer function model (which ignores mode shape information), the identification results are very satisfactory, characterized by only one misclassification error (test case 6).

The behavior of the geometric approach in conjunction with the deterministic metric and the Kullback pseudometric spaces is essentially identical, characterized by one misclassification error as well. The reason for this is the relatively low level of (purely numerical) noise present in the data in this setup, a fact reflected in the excessively high values of $Q(K)$ in test cases 1–16 (compare with the corresponding values of the beam experiment presented in Table 1) and the relatively small values of the estimated parameter covariance matrix (not shown).

V. Conclusions

A geometric approach to the nondestructive identification of faults in stochastic structural systems is presented. This approach overcomes many of the limitations of existing structural fault identification schemes because it effectively accounts for stochastic effects and the inherent variability of test data, requires a minimal number of measurement locations, is capable of operating on any type (acceleration, velocity, or displacement) of vibration test data, requires only partial (even single input/single output) and reduced-order models, and eliminates the difficulties associated with stiffness-matrix or modal-parameter-based procedures. The cost paid for these benefits is associated mainly with fault mode subspace construction, a procedure that, nevertheless, is implemented during the initial training stage. The geometric approach is, on the other hand, very general and potentially capable of identifying any type of fault within any linear or nonlinear structural system.

The effectiveness of the approach was demonstrated via fault identification in two structural systems: a laboratory-scale simply supported beam, and a finite element model of a planar truss structure. The importance of stochastic effect accommodation was, within this context, addressed, and the use of proper stochastic feature spaces was shown to be necessary in realistic cases in which environmental effects and noise (due to the experimental apparatus, modeling approximations, including the spatial and temporal model discretizations, and so on) cannot be neglected.

References

[1]Yao, J. T. P., "Identification of Structural Damage in Civil Engineering," *Application of System Identification in Engineering*, edited by H. G. Natke, Springer–Verlag, 1988, pp. 349–390.

[2]DiPasquale, E., Ju, J. W., Aksar, A., and Cakmak, A. S., "Relation Between Global Damage Indices and Local Stiffness Degradation," *Journal of Structural Engineering*, Vol. 116, 1990, pp. 1440–1456.

[3]Sanayei, M., and Onipede, O., "Damage Assessment of Structures Using Static Test Data," *AIAA Journal*, Vol. 29, 1991, pp. 1174–1179.

[4]Chen, J. C., and Garba, J. A., "On Orbit Damage Assessment for Large Space Structures," *Proceedings of the AIAA/ASME/ASCE/AHS 28th Structures, Structural Dynamics, and Materials Conference*, AIAA, New York, 1987, pp. 714–721.

[5]Smith, S. W., and Hendricks, S. L., "Evaluation of Two Identification Methods for Damage Detection in Large Space Structures," *Proceedings of the VPI and SU/AIAA 6th Symposium on Dynamics and Control of Large Structures*, AIAA, New York, 1987.

[6]Hemez, F. M., "Practical Guide to High Accuracy Identification of Structural Damage in Complex Structures," *Proceedings of the International Modal Analysis Conference* (Nashville, TN), 1995, pp. 1297–1304.

[7]Hajela, P., and Soeiro, F. J., "Structural Damage Detection Based on Static and Modal Analysis," *AIAA Journal*, Vol. 28, 1989, pp. 110–115.

[8]Wolff, T., and Richardson, M., "Fault Detection in Structures from Changes in Their Modal Parameters," *Proceedings of the International Modal Analysis Conference*, 1989, pp. 87–94.

[9]Shahrivar, F., and Bouwkamp, J. G., "Damage Detection in Offshore Platforms Using Vibration Information," *Journal of Energy Resources Technology*, Vol. 108, 1986, pp. 97–106.

[10]Hearn, G., and Testa, R. B., "Modal Analysis for Damage Detection in Structures," *Journal of Structural Engineering*, Vol. 117, 1991, pp. 3042–3063.

[11]Lew, J.-S., "Using Transfer Function Parameter Changes for Damage Detection of Structures," *AIAA Journal*, Vol. 33, No. 11, 1995, pp. 2189–2193.

[12]Söderström, T., and Stoica, P., *System Identification*, Prentice–Hall, Englewood Cliffs, NJ, 1989.

[13]Lee, J. E., and Fassois, S. D., "Suboptimum Maximum Likelihood Estimation of Structural Parameters from Multiple-Excitation Vibration Data," *Journal of Vibration and Acoustics*, Vol. 114, 1992, pp. 260–271.

[14]Fassois, S. D., and Lee, J. E., "On the Problem of Stochastic Experimental Modal Analysis Based on Multiple-Excitation Multiple-Response Data—Part II: The Modal Analysis Approach," *Journal of Sound and Vibration*, Vol. 161, 1993, pp. 57–87.

[15]Draper, N. R., and Smith, H., *Applied Regression Analysis*, 2nd ed., Wiley, New York, 1981.

[16]Kullback, S., *Information Theory and Statistics*, Wiley, New York, 1959.

[17]Rao, S. S., *Optimization: Theory and Application*, Wiley, New York, 1984.

[18]Cook, R. D., Malkus, D. S., and Plesha, M. E., *Concepts and Applications of Finite Element Analysis*, Wiley, New York, 1989.

A. M. Waas
Associate Editor